3D Simulation of the Defect Generation by Hydrogen at $Si - SiO_2$ Interface

***Zhaocan Ma**[1], **Jingjie Xu**[1], **Hongliang Li**[2], **Song Yu**[2], **Linbo Zhang**[1], and **†Benzhuo Lu**[1]

[1] *State Key Laboratory of Scientific and Engineering Computing, Academy of Mathematics and Systems Science, Chinese Academy of Sciences, Beijing, China*
[2] *Microsystem & Terahertz Research Center, China Academy of Engineering Physics, Chengdu, China*
* *Presenting author: zhaocanma@lsec.cc.ac.cn*
† *Corresponding author: bzlu@lsec.cc.ac.cn*

Abstract

In order to study defect generation and radiation-induced interface in semiconductor influenced by dose rate response and H_2, we provide a 3D finite element model based on Poisson-Nersnt-Planck equations to simulate the electro-diffusion process in numerical experiment. Multi-scale method is used in discretization and the restricted additive Schwarz preconditioner is applied to solve the linear system in simulation. The algorithm we establish in this work is solved by our parallel finite element software based on Parallel Hierarchical Grid with high efficiency. It is shown that the numerical results from our simulation agree well with experimental data of the devices affected by enhanced low dose-rate sensitivity in different H_2 environments.

Keywords: defect generation, $Si - SiO_2$ interface, enhanced low dose-rate sensitivity (EDLRS), multi-scale method.

Introduction

Total ionizing dose (TID) effect is well known as the results of generating charges in semiconductor devices designing for the space environment. As reported in previous work, [7] degradation of bipolar device characteristics increases at low dose rates irradiation, and this phenomenon is referred as enhanced low dose-rate sensitivity (ELDRS). ELDRS has great effect on modern silicon devices, and it is observed to be strongly related to hydrogen. For hermetically sealed integrated circuits (ICs) used in satellites and other space-based systems in radiation environments, the presence of high concentrations of H_2 in the package can enhance radiation-induced degradation, which greatly reduces their operation reliability. Bulk oxide (like SiO_2) and interface defects play an important role as charge trapping sites. When radiation induced, the SiO_2 layers of the device is charged and the interface traps N_{it} at the Si/SiO_2 interface increase (see Figure 1). Once this situation occurs, subsequent physical effects, such as the changing of threshold voltage, will disturb the working state of devices. After plenty of experiments, several models have been proposed to describe the phenomenon. [5] [11] [12] However, these models are

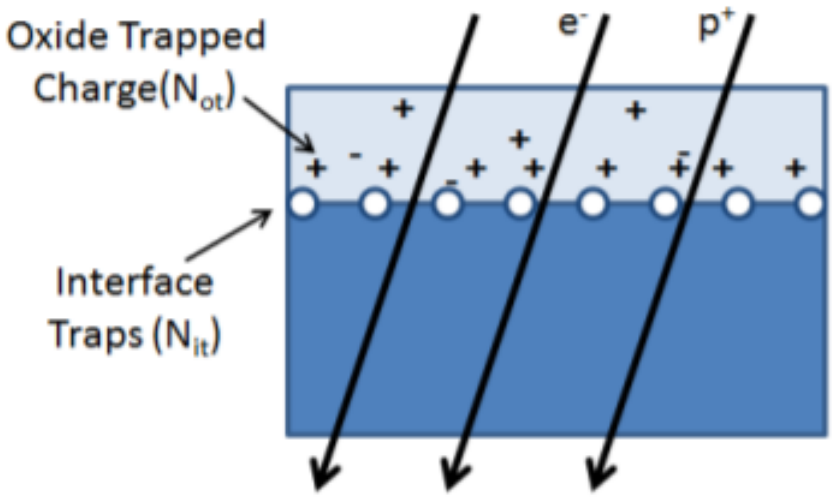

Figure 1: An illustration showing ionizing dose in SiO_2-on-Si structures.

limited in 1D or 2D cases with low efficiency [9].

In this paper, we recalculate the same Poisson-Nernst-Planck (PNP) model studied by Nicole L. Rowsey [12] with a new 3D numerical simulation, which is more complex and reasonable in describing the coupling of potential field and diffusion processes. We solve the PNP equations by finite element method, just as the numerical simulations of biochemical systems in previous works. [16][17][14] However, various simulated species along with the electrostatic voltage are considered in the model, some of which are extremely sensitive to time scale, so that the multi-scale method is an optional choice in our simulation. In addition, restricted additive Schwarz preconditioner[2] is used to solve the linear systems generated in diffusion-convection equations with high efficiency. As computations increase rapidly in 3D model compared to previous cases, we develop a parallel software to reduce the cost of simulation time. The parallel efficiency is presented in "Parallel Efficiency" section.

Drift-Diffusion Modeling

Trapping Species

Oxygen vacancies are the dominant defects in SiO_2 [1]. The neutral oxygen vacancy includes one $Si-Si$ bond instead of two $Si-O$ bonds. Because of the distinct energies, There are two detect species, detects $V_{o\delta}^{+}$ and $V_{o\gamma}^{+}$, and two neutral precursors, $V_{o\delta}$ and $V_{o\gamma}$. It is shown by observing the associated energies that $V_{o\delta}^{+}$ is a shallow hole trap, while $V_{o\gamma}^{+}$ is much deeper. These two kinds of defects can be hydrogenated or doubly hydrogenated to form $V_{o\gamma}H$, $V_{o\gamma}H^{+}$, $V_{o\gamma}H_2$, $V_{o\gamma}H_2^{+}$, $V_{o\delta}H$, $V_{o\delta}H^{+}$ and $V_{o\delta}H_2$, $V_{o\delta}H_2^{+}$, respectively.

Chemical Reactions

Here, we briefly summarize the influences of radiation-induced electrons and holes on metal-oxide-semiconductor (MOS) structures.

- Radiation emerges Electron-hole pairs (EHPs).

- The electric field pushes holes escaping initial recombination towards the interface, while electrons are towards the metal gate.
- Neutral oxygen vacancies become positively charged when capturing holes and then are neutralized by electrons.
- Protons and hydrogenated defects are created when molecular hydrogen recombines the positively charged defects.
- Protons can also be cracked by positively-charged hydrogenated defects directly.
- Interface traps are formed by the react of protons and the $Si-H$ bonds on the SiO_2/Si interface.

$$H^+ + Si - H \Leftrightarrow N_{it} + H_2 \tag{1}$$

Poisson-Nernst-Planck Equations

In this model, every kind of species participates in chemical reactions and therefore we use generation and recombination terms in Nernst-Planck equation to simulate the ion transport process. The electrostatic field is determined by applied voltage and charged species, including electron-hole pairs (EHPs) and positively charged defects, which are simulated by Poisson equation shown as follows:

$$\epsilon \nabla^2 \phi = -Q \tag{2}$$

$$Q_{SiO_2} = q(p + H^+ + V_{o\delta}^+ + V_{o\delta}H^+ + V_{o\delta}H_2^+ + +V_{o\gamma}^+ + V_{o\gamma}H^+ + V_{o\gamma}H_2^+ - n) \tag{3}$$

Electrons, holes and H^+ are charged and mobile, so the diffusion-convection process is considered. The $U_{radiation}$ is the EHP generation term [10]. During the radiation, recombination and generation of spices also arise by the chemical reactions, and they must also be accounted in the continuity equations, which we will describe later.

$$\frac{\partial n}{\partial t} = \nabla \cdot (e\mu_n nE + D_n \nabla n) + U_{radiation} + G_n - R_n \tag{4}$$

$$\frac{\partial p}{\partial t} = -\nabla \cdot (e\mu_p pE - D_p \nabla p) + U_{radiation} + G_p - R_p \tag{5}$$

$$\frac{\partial H^+}{\partial t} = -\nabla \cdot (e\mu_{H^+} H^+ E - D_{H^+} \nabla H^+) + G_{H^+} - R_{H^+} \tag{6}$$

Hydrogen is mobile, but not charged.

$$\frac{\partial H_2}{\partial t} = D_{H_2} \nabla H_2 + G_{H_2} - R_{H_2} \tag{7}$$

The defects including $V_{o\gamma}, V_{o\gamma}^+, V_{o\delta}, V_{o\delta}^+, V_{o\gamma}H, V_{o\gamma}H^+, V_{o\delta}H, V_{o\delta}H^+, V_{o\gamma}H_2, V_{o\delta}H_2, V_{o\gamma}H_2^+, V_{o\delta}H_2^+$ are not mobile with no drift nor diffusion, but they still have recombination and generation terms.

$$\frac{dT_i}{dt} = G_i - Ri \tag{8}$$

Recombination and Generation Terms

As the chemical reactions are complicate, we use recombination and generation terms to stand for chemical reactions in PNP equations, and these terms are nonzero after irradiation. Consider the bulk reactions:

$$A + B \Leftrightarrow C \qquad (Reaction \quad 0)$$
$$A + M \Leftrightarrow C + N \qquad (Reaction \quad 1)$$

For non-equilibrium conditions, each specie has recombination and generation terms, we take spice A for example, whose rates have the following form:

- the generation term of A can be described as:

$$G_A = k_{r_0} \cdot [C] + k_{r_1} \cdot [C][N]$$

- the recombination term of A can be described as:

$$R_A = k_{f_0} \cdot [A] \cdot [B] + k_{f_1} \cdot [A] \cdot [M]$$

where k_f and k_r are reaction rates; the bracket represents concentration of the species in $/cm^3$. The recombination and generation terms of other spices can be defined as the same.

Then we can add the recombination and generation terms to each continuity equation. The reaction rates k_f, k_r are formulated in 3 different cases, which can be found in Ref.[13].

Boundary Conditions

Here we describe the boundary conditions of mobile particles. On the gate contact and SiO_2/Si interface, Electron, holes and protons are allowed to move freely. For H_2 case, there are two possible choices depending on whether the edge is exposed or shielded.

1 Exposed case: H_2 concentration on the gate is constant and equals to the ambient concentration but reflection boundary condition on the interface.

2 Non-exposed case: reflection boundary condition on both edges.

For the surrounding edges of the SiO_2 bulk, all moving particles have reflection boundaries.
H^+ has to be emphasized on Si/SiO_2 interface because of the reaction:

$$H^+ + Si - H \Leftrightarrow N_{it} + H_2$$

The reverse reaction is negligible at room temperature and we can give the continuity equation of interface traps:

$$\frac{dN_{it}}{dt} = k_{int} \cdot [H^+]_{int}[SiH]_{int} \tag{9}$$

Since the $[H^+]_{int}, [SiH]_{int}$ is 2D with the unit of$/cm^2$ on the interface, we present the equation in another form as in Ref. [8].

$$\frac{dN_{it}}{dt} = \sigma_{int}\vec{J}_{H^+} \cdot \vec{n}([SiH] - [Nit]) \tag{10}$$

σ_{int} is the transformation coefficient with the unit of cm^2

Multi-scale Methods

Finite Element Method is used to spatially discrete the PNPs with generation and recombination terms and backward Euler method is applied to discrete the time step. Actually, the reaction process is an ODE problem, since some particles are sensitive about time.

Take $V_{o\gamma}H_2^+$ for example:

$$\begin{aligned}\frac{dV_{o\gamma}H_2^+}{dt} =&(1.03e-13)[V_{o\gamma}H_2][h^+]+(1.03e-19)[V_{o\gamma}][H^+]+(4.02e-21)[V_{o\gamma}^+][H_2]\\ &+(3.21e-138)[V_{o\gamma}H_2]\\ &-(4.16e+3)[V_{o\gamma}H_2^+]-(3.81e+5)[V_{o\gamma}H_2^+]-(1.90e+5)[V_{o\gamma}H_2^+]\\ &-(2.06e-07)[V_{o\gamma}H_2^+][e^-]\end{aligned} \tag{11}$$

Some parameter can be regarded as 0. And we can simplify it as:

$$\frac{\partial V_{o\gamma}H_2^+}{\partial t} = -O(10^5)V_{o\gamma}H_2^+ + C \tag{12}$$

To get this equation solved, the time step should be less than $10^{-5}s$. During the simulation, if we choose a time step that small, considering the amount of irradiation, it will take too much time at this time scale.

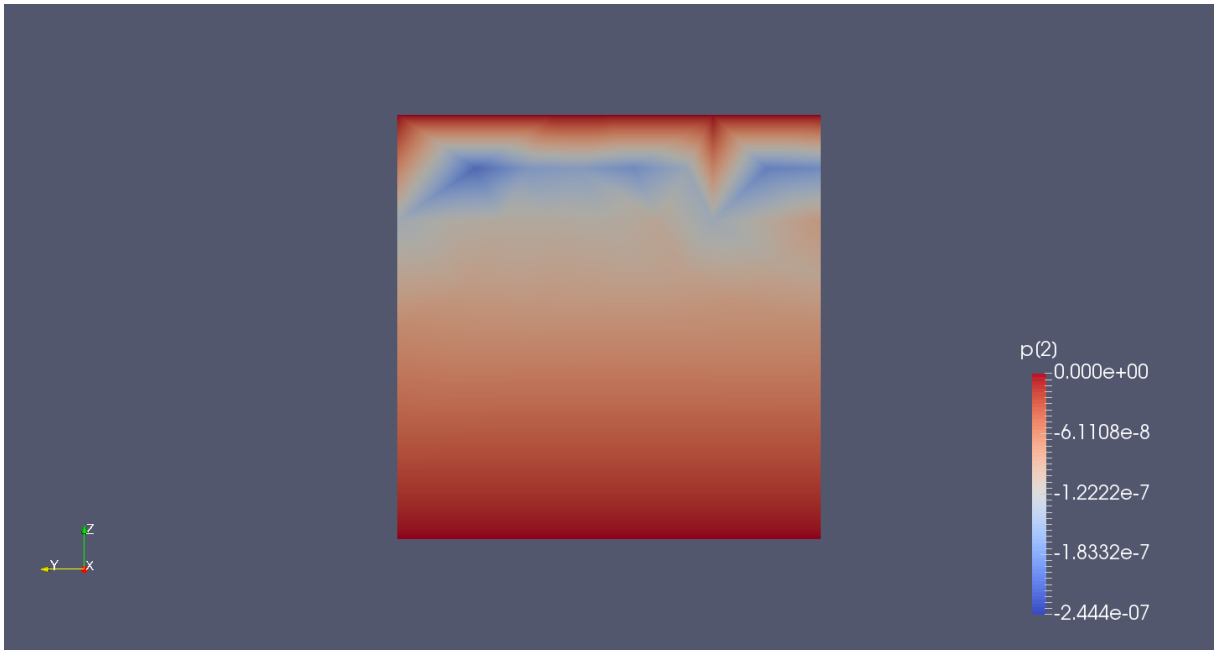

Figure 2: Distribution of H^+ without multi-scale method

So we explore a kind of multi-scale method to overcome the problem. We firstly set drift and diffusion terms as the macro-variable reaction parameters, like e^-, h^+, H^+, H_2. The detects, that can't move, treat as the micro-variable, like $V_{o\gamma}, V_{o\delta}$, then we can give the algorithm:

- Step 1. Given the current state of the reaction parameters, initialize the macro-variable of e^-, h^+ using the macro-solver with generating terms and reaction terms, and take their results as current state;

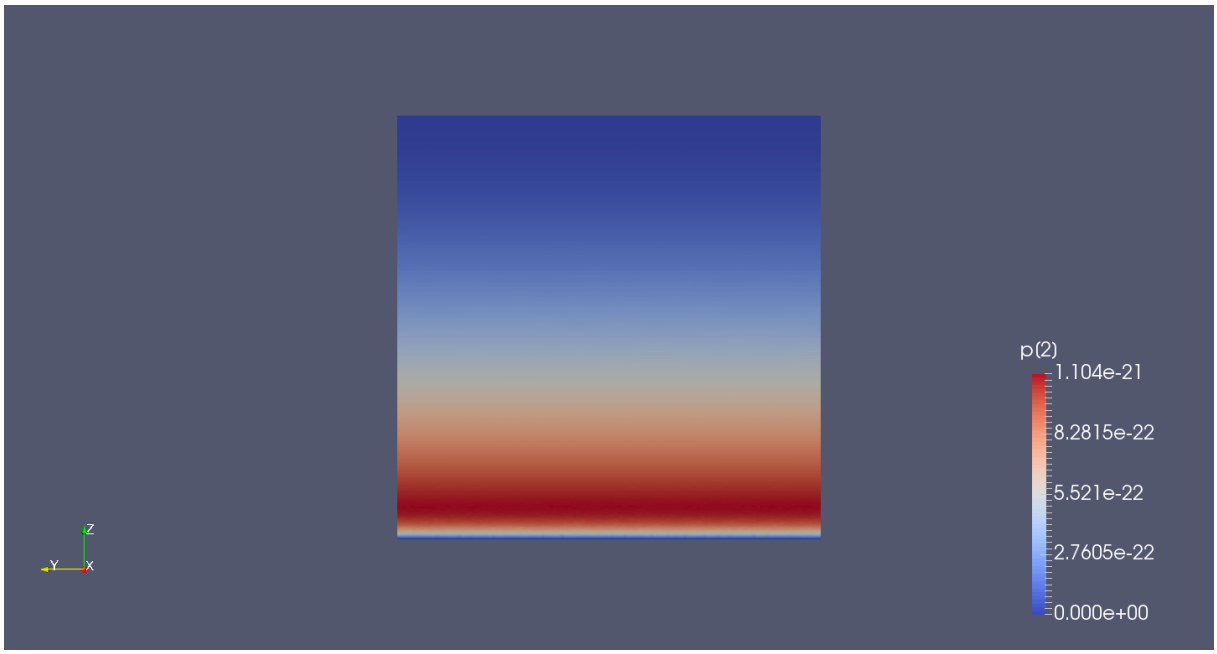

Figure 3: Distribution of H^+ with multi-scale method

- Step 2. Evolve the micro-variables like $V_{o\gamma}, V_{o_\delta}$ for M micro time steps with iteration method like Euler method using the current step of e^-, h^+ to ensure the convergence;

$$\frac{c_i^{n+1} - c_i^n}{\delta t} = G_i^n - R_i^n \quad (n = 0, ..., M-1) \tag{13}$$

- Step 3. Estimate the generating terms and reaction terms of other macro variables and evolve the macro-variable of H^+, H_2 for one macro time step using the macro-solver;

- Step 4. Set the current state of the macro-variables and repeat

We choose restricted additive Swcharz precondioner in Ref.[2] and GEMRS method as macro-solver to get the solutions, which will improve the parallel efficiency comparing with regular additive Schwarz precondioner.

As suggested above, in order to accelerate the simulation, we implement the multi-scale algorithm to calculate the time-dependent Nersnt-Planck equation. The difference of result between the two algorithms, with and without multi-scale method, is shown in Figure 2 and Figure 3.

Numerical Results

H_2 *Trend*

For different kind of semiconductor, the doping situation changes. And the difficulties of simulation are different, since the linear system of high doping case is much more singular to solve. We present two different doping parameters in Table 1. Considering the time cost is very expensive even with the parallel method, we have to try the total dose of 0.1krad, which is less than the experiment. Every point we get need nearly 3000s, but it

is still much faster than other simulation time [9]. The mesh we use to calculate below has 168986 vertices and 977221 tetrahedra. Figure 4 shows the trend of N_{it} data in different H_2 concentrations, which matches the data taken by the experiments [5]. The high doping case has a swift change despite the similar trend, which could be explained by the cracking of double-hydrogenated defects.

Table 1: Semiconductor with different doping [15] [6]

parameters	low doping	high doping
H_2	$10^{11} - 10^{18} cm^{-3}$	$10^{11} - 10^{18} cm^{-3}$
$V_{o\gamma}$	$1.0e14 cm^{-3}$	$1.0e15 cm^{-3}$
$V_{o\delta}$	$1.0e18 cm^{-3}$	$1.0e18 cm^{-3}$
$V_{o\gamma}H$	$1.0e14 cm^{-3}$	$1.0e14 cm^{-3}$
$V_{o\delta}H$	$1.0e14 cm^{-3}$	$1.0e14 cm^{-3}$
$V_{o\gamma}H_2$	$1.0e14 cm^{-3}$	$1.0e16 cm^{-3}$
$V_{o\delta}H_2$	$1.0e13 cm^{-3}$	$1.0e16 cm^{-3}$
$Si - H$	$1.0e13 cm^{-2}$	$1.0e13 cm^{-2}$

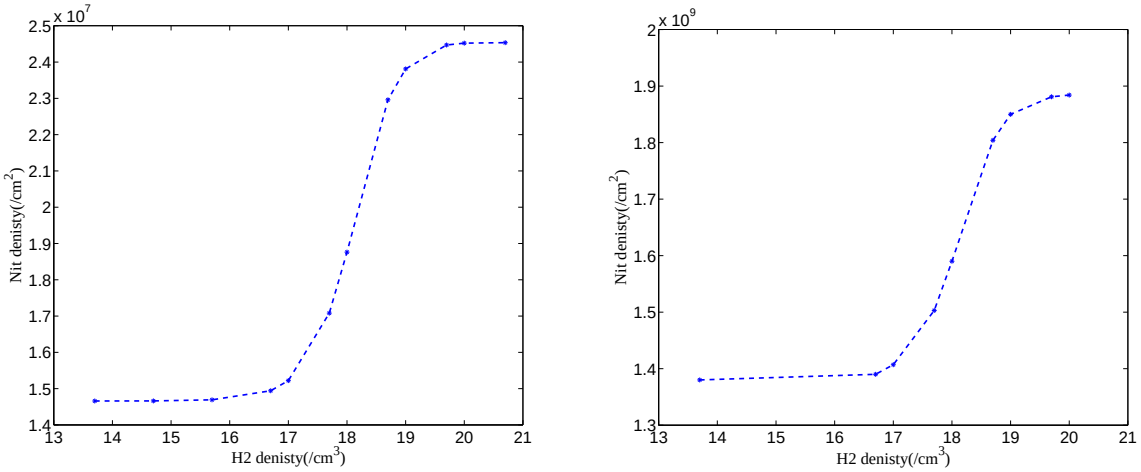

Fig.a Fig.b

Figure 4: Total dose of 0.1krad with 10rad/s in low doping (Fig.a) and high doping(Fig.b)

EDLRS Effect

We also simulate the EDLRS response in Figure 5 and show the general expected trend which matchs the trend of experiment data [11] and the simulation result of 1D case [4]. The quantities of interface traps reduce by the increase of dose rate and we predict to raise the amount of total dose and present better characterization in our later work.

Parallel Efficiency

Here we present parallel efficiency results. The implementation of the algorithm is based on the package PHG [18], which is a parallel toolbox for writing adaptive finite element programs. In order to assess the parallel scalability and efficiency with 1024 processes,

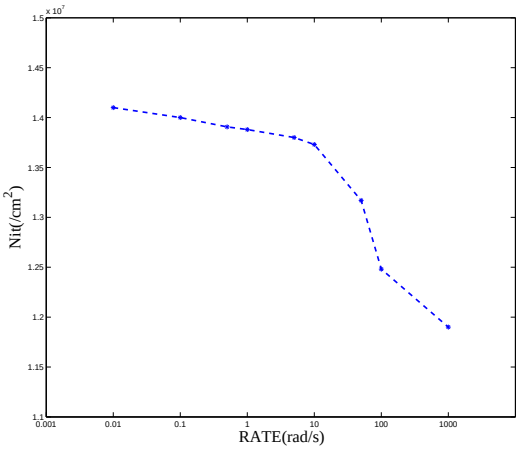

Figure 5: Total dose of 0.1krad and the H2 density of $3e14cm^{-3}$

we simulate a much larger system with a mesh containing 1418778 vertices and 8637254 tetrahedra, as MPI communication costs too much time in small system. We use GMRES method with restricted additive Schwarz preconditioner as our linear system solver. Table 4 gives the wall-clock time and parallel efficiency for different amount of MPI processes. Considering the large memory requirement, our tests start with 32 processes, whose parallel efficiency is regarded as 100%, and the parallel efficiency for p processes can be defined as:

$$E_p = \frac{32T_{32}}{pT_p}$$

where T_p denotes the time to irradiate 0.1krad with the rate of 10 rad/s for solving the PNPEs using p processes. In most cases, it proves that our method has good parallel scalability.

Table 2: parallel extendiability

Num of procs	Times	Efficiency
32	182000s	100%
64	75888s	120%
128	30444s	149%
256	16566s	137%
512	14570s	78%

Conclusion

We have developed a parallel finite element code to give a glimpse at the TID effects. The parallel solution of time-dependent PNP equations with reaction functions have been explored. During the simulation, multi-scale method is presented to dispose the time scale sensitive parameters and restricted additive Schwarz preconditioner is used to overcome the singularity of linear system. Our result shows a good match with the influence of H_2 concentration and dose rate. Further study will focus on the error estimate and reducing calculation time.

Acknowledgement

All the authors are supported by Science Challenge Program (SCP JCKY2016212A503) and the China NSF (NSFC 21573274).

References

[1] Peter E Blöchl. First-principles calculations of defects in oxygen-deficient silica exposed to hydrogen. *Physical Review B*, 62(10):6158, 2000.

[2] Xiao Chuan Cai and Marcus Sarkis. A restricted additive schwarz preconditioner for general sparse linear systems. *Siam Journal on Scientific Computing*, 21(2):792–797, 1999.

[3] Tony F Chan and Tarek P Mathew. Domain decomposition algorithms. *Acta numerica*, 3:61–143, 1994.

[4] X. J Chen, H. J Barnaby, P Adell, and R. L Pease. Modeling the dose rate response and the effects of hydrogen in bipolar technologies. *IEEE Transactions on Nuclear Science*, 56(6):3196–3202, 2010.

[5] X. J. Chen, H. J. Barnaby, B. Vermeire, and K. Holbert. Mechanisms of enhanced radiation-induced degradation due to excess molecular hydrogen in bipolar oxides. *IEEE Transactions on Nuclear Science*, 54(6):1913–1919, 2007.

[6] RAB Devine, D Mathiot, WL Warren, DM Fleetwood, and B Aspar. Point defect generation during high temperature annealing of the si-sio2 interface. *Applied physics letters*, 63(21):2926–2928, 1993.

[7] E. W. Enlow, R. L. Pease, W. Combs, and R. D. Schrimpf. Response of advanced bipolar processes to ionizing radiation. *IEEE Transactions on Nuclear Science*, 38(6):1342–1351, 1991.

[8] Ivan Sanchez Esqueda. *Modeling of total ionizing dose effects in advanced complementary metal-oxide-semiconductor technologies*. PhD thesis, Arizona State University, 2011.

[9] Harold P. Hjalmarson, Ronald L. Pease, and Roderick A. B. Devine. Calculations of radiation dose-rate sensitivity of bipolar transistors. *IEEE Transactions on Nuclear Science*, 55(6):3009–3015, 2008.

[10] Timothy R Oldham. *Ionizing radiation effects in MOS oxides*. World Scientific, 2000.

[11] Ronald L. Pease, Philippe Claude Adell, Bernard G. Rax, and Xiao Jie Chen. The effects of hydrogen on the enhanced low dose rate sensitivity (eldrs) of bipolar linear circuits. *IEEE Transactions on Nuclear Science*, 55(6):3169–3173, 2008.

[12] N. L Rowsey, M. E Law, R. D Schrimpf, and D. M Fleetwood. A quantitative model for eldrs and degradation effects in irradiated oxides based on first principles calculations. *Nuclear Science IEEE Transactions on*, 58(6):2937–2944, 2011.

[13] Nicole L Rowsey. *Quantitative modeling of total ionizing dose reliability effects in device silicon dioxide layers*. 2012.

[14] Bin Tu, Minxin Chen, Yan Xie, Linbo Zhang, Bob Eisenberg, and Benzhuo Lu. A parallel finite element simulator for ion transport through three-dimensional ion channel systems. *Journal of computational chemistry*, 34(24):2065–2078, 2013.

[15] WL Warren, DM Fleetwood, MR Shaneyfelt, JR Schwank, PS Winokur, RAB Devine, and D Mathiot. Links between oxide, interface, and border traps in high-temperature annealed si/sio2 systems. *Applied physics letters*, 64(25):3452–3454, 1994.

[16] Yan Xie, Jie Cheng, Benzhuo Lu, and Linbo Zhang. Parallel adaptive finite element algorithms for solving the coupled electro-diffusion equations. *Molecular Based Mathematical Biology*, 1:90–108, 2013.

[17] Jingjie Xu, Yan Xie, Benzhuo Lu, and Linbo Zhang. Charged substrate and product together contribute like a nonreactive species to the overall electrostatic steering in diffusion-reaction processes. *The Journal of Physical Chemistry B*, 120(33):8147–8153, 2016.

[18] Lin-Bo Zhang. A parallel algorithm for adaptive local refinement of tetrahedral meshes using bisection. *Numer. Math.: Theory, Methods and Applications*, 2:65–89, 2009.